EFFECT OF BASELINE ON STEREO VISION SYSTEMS

A Project

Presented to the faculty of the Department of Electrical and Electronic Engineering

California State University, Sacramento

Submitted in partial satisfaction of
the requirements for the degree of

MASTER OF SCIENCE

in

Electrical and Electronic Engineering

by

Kexian Shen

SPRING
2018

EFFECT OF BASELINE ON STEREO VISION SYSTEMS

A Project

by

Kexian Shen

Approved by:

_____, Committee Chair
Fethi Belkhouche, Ph.D.

_____, Second Reader
Preetham Kumar, Ph.D.

_____
Date

Student: Kexian Shen

I certify that this student has met the requirements for format contained in the University format manual, and that this project is suitable for shelving in the Library and credit is to be awarded for the project.

_____, Graduate Coordinator _____
Preetham Kumar, Ph.D. Date

Department of Electrical and Electronic Engineering

Abstract

of

EFFECT OF BASELINE ON STEREO VISION SYSTEMS

by

Kexian Shen

Stereo vision systems imitate the mechanisms of natural human vision to get three-dimension information from captured scenes. It is applied in the control of autonomous robots (to build a map of the environment) and the control of production tools. Stereo systems are deployed to identify objects and can be used for determining close-range depth. However, the error in estimated depth grows quadratically with the real depth. To increase accuracy, we must adjust the focal length and the baseline. Most cameras' focal lengths are flexible to suit different scenes. However, once the baseline is fixed, it is inconvenient to change. Therefore, finding a suitable baseline is vital when designing a stereo vision system.

To find the relationship between baseline and depth accuracy, the accuracy estimation needs to be analyzed based on stereo vision model and error propagation. Meanwhile, a measurement experiment will be conducted to confirm the relationship.

The image data used in this project are captured by two GoPro cameras. Camera calibrations, as well as image operations and calculations are conducted using MATLAB.

The accuracy of estimation is analyzed, which shows a simple relationship between accuracy and baseline. Based on this relationship, it is easy to determine a suitable baseline for different applications.

_____, Committee Chair
Fethi Belkhouche, Ph.D.

_____
Date

ACKNOWLEDGEMENTS

There are many people I would like to thank for the help they offering to accomplish my project, my advisor Prof. Belkhouche, my friends, and family.

I am glad that I chose Prof. Belkhouche to be my advisor one year ago. Since then, I enrolled in Machine Vision (EEE221) and Control (EEE241), which helped me find a job in an automobile company to do coding work on auto driving.

Finally, I would like to thank my friends and family, especially Hao Wu, who help me deliver paper materials when I am not in the United States, and Zhicheng Guo, who assisted me conducting the capturing work. This project would not have been accomplished without their help.

TABLE OF CONTENTS

Page

LIST OF TABLES

Tables Page

LIST OF FIGURES

Figures Page

CHAPTER 1

INTRODUCTION

1.1. Background of the Project

Stereo vision is an important branch of the field of Computer Vision. It simulates the mechanisms of natural human vision to sense the three-dimensional world. Stereo vision is widely applied in many fields, such as vision-based control of machines, three-dimension non-contact object measurement, visual or digital reconstruction of surfaces and so on. Thanks to the accelerated computing ability, real-time 3D measurement, and 3D scene reconstruction became possible. In autonomous cars, stereo systems are deployed to identify objects [1] and can be used for determining close-range depth. Due to low cost and passive-receiving, stereo vision systems are becoming a promising component of self-driving vehicles' perception.

To improve the accuracy of measurement through stereo vision systems, accurate camera calibration and suitable system structure are essential elements. In stereo vision systems, the baseline and the focal length are two important parameters [2], which dominate the measurement error. Meanwhile, in most applications, cameras' focal lengths are flexible to suit different scenes. But baselines are fixed or inconvenient to change. Therefore, finding a suitable baseline is critical when designing a stereo vision system.

1.2. Goal of the Project

The goal of this project is to find the relationship between baseline and accuracy in stereo vision systems. To achieve this goal, measurement error is analyzed based on measurement equations and error propagation rules. Then to confirm the relationship, a measurement

experiment was conducted, where two GoPro cameras were calibrated and used to build a stereo vision system. After stereo calibration and image pair rectification, the depth, which is the distance between the object of interest and the stereo cameras, was calculated based on x-parallax. Then the dimension of the detected object can be calculated from the depth. For simplicity, only the object's vertical length (height) was calculated and compared with the real value to confirm and validate the results.

1.3. Layout of the Project

This report is organized as follows: Chapter 2 presents the stereo vision basics. Error analysis based on measurement equations and error propagation rules are shown in chapter 3. The methodology of the experiment is illustrated in chapter 4. Experimental results and analysis are presented in chapter 5. Conclusions and future work are presented in chapter 6.

CHAPTER 2

STEREO VISION

2.1. Pinhole Camera Model

The pinhole camera model establishes an approximated one-to-one mapping between the 3D object and the 2D image, as shown in Fig. 1.

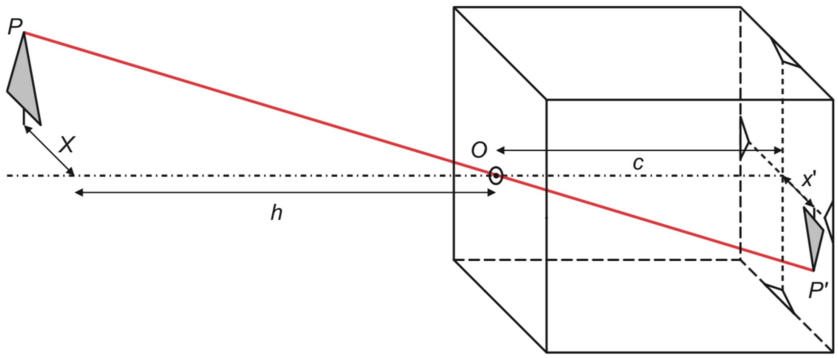

Figure 1. Pinhole camera model

The plane (on the right of the box) is commonly called the image plane. The aperture on the box is called pinhole or camera center, through which all the image rays pass. The distance between the image plane and the camera center is the focal length typically denoted by c or f. The 3D point P = [x y z] in Fig. 1 is projected into a point P' = [x' y'] in the image plane. The relationship between P and P' is shown in equation (1), it is derived using similar triangles properties.

$$\begin{cases} x' = c\dfrac{x}{h} \\ y' = c\dfrac{x}{h} \end{cases} \tag{1}$$

The general pinhole camera model [3] is:

$$P' = K\begin{bmatrix} R & T \end{bmatrix} P = MP \tag{2}$$

$$K = \begin{bmatrix} \alpha_u & -\alpha\cot\theta & u_0 \\ 0 & \dfrac{\alpha_v}{\sin\theta} & v_o \\ 0 & 0 & 1 \end{bmatrix} \tag{3}$$

Here matrix K is called the camera intrinsic matrix; θ is the skew angle; α_u is focal length divided by pixel's horizontal dimension; α_v is focal length divide d by pixel's vertical dimension; u_0, v_o are the principle point's offsets. Note that α_u and α_v do not have a unit.

It is possible to write

$$R = \begin{bmatrix} r_1^T \\ r_2^T \\ r_3^T \end{bmatrix} \tag{4}$$

$$T = \begin{bmatrix} t_x \\ t_y \\ t_z \end{bmatrix} \tag{5}$$

where rotation matrix R is 3×3 and translation vector T is 3×1. R and T together form the extrinsic parameters of the camera. It is possible to combine the intrinsic and extrinsic parameters of the camera as follows:

$$M = K\begin{bmatrix} R & T \end{bmatrix} = \begin{bmatrix} \alpha_u r_1^T - \alpha_u\cot\theta r_2^T + u_0 r_3^T & \alpha_u t_x - \alpha_u\cot\theta t_y + u_0 t_z \\ \dfrac{\alpha_v}{\sin\theta} r_2^T + v_o r_3^T & \dfrac{\alpha_v}{\sin\theta} t_y + v_o t_z \\ r_3^T & t_z \end{bmatrix}_{3\times4} \tag{6}$$

2.2. Stereo Vision Basics

Stereo vision refers to the acquisition of images from a pair of cameras, which are usually mounted on a stable base bar.

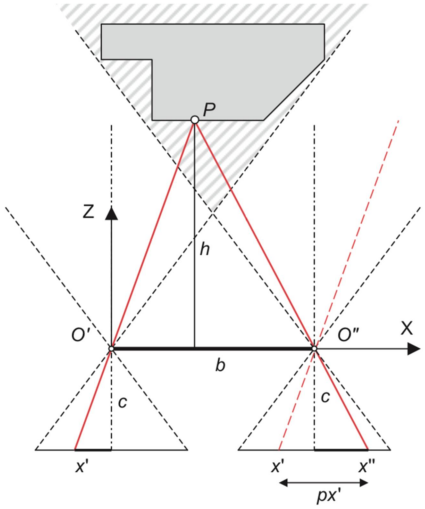

Figure 2. Stereo vision geometry

Camera geometry for stereo vision is shown in Fig. 2, where O' and O'' are the centers of two cameras; b defines the baseline between the two cameras; c is the focal length. Using similar triangles properties, we get [2]:

$$Z = h = \frac{bc}{x' - x''} = \frac{bc}{px'} \tag{7}$$

where $x' - x''$ or x_p is called x-parallax.

Equation (7) shows how to calculate the depth information using a simplified model assuming identical cameras and no rotation or translation between the cameras.

2.3. Modified Stereo Model

Assuming that stereo images have been undistorted and rectified and the translation vector T is expressed as $T = \begin{bmatrix} b & d & e \end{bmatrix}^T$, the measurement equation (7) can be modified as:

$$Z = \frac{b - \frac{x''e}{c_r}}{\frac{x'}{c_l} - \frac{x''}{c_r}} \tag{8}$$

It is possible to rewrite equation (8) by converting distances to pixels:

$$Z = \frac{b - \frac{\left(r_r - u_{0r}\right)s_{xr}e}{c_r}}{\frac{\left(r_l - u_{0l}\right)s_{xl}}{c_l} - \frac{\left(r_r - u_{0r}\right)s_{xr}}{c_r}} = \frac{b - \alpha_{ur}r_r e + \alpha_{ur}u_{0r}e}{\alpha_{ul}r_l - \alpha_{ur}r_r - \alpha_{ul}u_{0l} + \alpha_{ur}u_{0r}} \tag{9}$$

$$\begin{cases} X = \frac{r_l - u_{0l}}{\alpha_{ul}} Z \\ Y = \frac{c_l - v_{0l}}{\alpha_{vl}} Z \end{cases} \tag{10}$$

where,

- (r_l, c_l) is point P's projection in pixel coordinates of left image plane.
- (r_r, c_r) is point P's projection in pixel coordinates of right image plane.
- α_{ul} is left camera's focal length divided by pixel's horizontal dimension.
- α_{ur} is right camera's focal length divided by pixel's horizontal dimension.
- α_{vl} is left camera's focal length divided by pixel's vertical dimension.
- u_{0l} is the r-axis coordinate of the left camera's principle point.
- u_{0r} is the r-axis coordinate of the right camera's principle point.
- v_{0l} is the c-axis coordinate of the left camera's principle point.

CHAPTER 3

THEORETICAL ANALYSIS OF ACCURACY

3.1. Theoretical Analysis of Accuracy

Differentiation of equation (7) and application of error propagation gives the following accuracy estimation of the object coordinate in the z-axis direction [4]:

$$s_Z = -\frac{bc}{px'^2} s_{px'} \tag{11}$$

By subtracting px' according to equation (7), we have:

$$s_Z = \frac{Z^2}{bc} s_{px'} = \frac{Z}{b}\frac{Z}{c} s_{px'} \tag{12}$$

Here $s_{px'}$ defines the image measurement precision of the x-parallax; baseline b and focal length c are assumed to be free of error. Equation (12) shows that the accuracy in the z-axis direction depends on the image scale (Z/c) and the depth-to-base ratio (Z/b). Since b and c are constant for one particular case, the accuracy drops in proportion to the square of the depth Z.

By rearranging equation (12), the error percentage ratio is:

$$\frac{S_Z}{Z} = \frac{Z}{bc} s_{px'} \tag{13}$$

For example, if the focal length of two identical cameras is 21mm; the cameras are calibrated at pixel-level; the horizontal dimension of a pixel is 1.2×10^{-5} m; the baseline is 0.5m; the true distance between object and cameras is 100m, then the error percentage ratio of the measured distance is $100\times1.2\times10^{-5}/0.5\times21\times10^{-3} = 11.4\%$.

Equation (13) shows that to satisfy a specific accuracy, we should choose cameras with suitable focal length and have the right baseline between them. Meanwhile, sub-pixel level

calibration is highly recommended for improving image measurement precision. With good sub-pixel level calibration, lenses with reasonably short focal length can be chosen and used.

3.2. Theoretical Analysis of Accuracy in Modified Model

The modified model is more general. According to error propagation rules [4], the accuracy estimation of the object coordinate in the z-axis direction is derived as follows (assuming camera intrinsic and extrinsic parameters are free of error):

$$s_Z = \sqrt{\left(\frac{\partial Z}{\partial x'} s_{x'}\right)^2 + \left(\frac{\partial Z}{\partial x''} s_{x''}\right)^2} \tag{14}$$

where, s_Z is the measurement accuracy of the Z coordinate; $s_{x'}$ and $s_{x''}$ represent two cameras' image measurement precision of the X-axis direction in the pixel coordinates. They do not depend on each other. Otherwise, equation (14) is not suitable based on error propagation rules.

Differentiation of equation (8) gives the following equations:

$$\begin{cases} \dfrac{\partial Z}{\partial x'} = \dfrac{\dfrac{x''e}{c_l c_r} - \dfrac{b}{c_l}}{\left(\dfrac{x'}{c_l} - \dfrac{x''}{c_r}\right)^2} \\ \dfrac{\partial Z}{\partial x''} = \dfrac{-\dfrac{x'e}{c_l c_r} + \dfrac{b}{c_r}}{\left(\dfrac{x'}{c_l} - \dfrac{x''}{c_r}\right)^2} \end{cases} \tag{15}$$

Here c_l is the left camera's focal length; c_r is the right camera's focal length; b and e are the first and the third components of the translation vector T.

CHAPTER 4

EXPERIMENT METHODOLOGY

4.1. Camera Calibration Based on Linear Model

The goal of camera calibration is to estimate the intrinsic and extrinsic parameters. From equation (2), we have

$$p_i = \begin{bmatrix} u_i \\ v_i \end{bmatrix} = \begin{bmatrix} \dfrac{m_1 P_i}{m_3 P_i} \\ \dfrac{m_2 P_i}{m_3 P_i} \end{bmatrix} \tag{16}$$

where $\mathrm{M} = \begin{bmatrix} \mathrm{m}_1 \\ \mathrm{m}_2 \\ \mathrm{m}_3 \end{bmatrix}$; $\mathrm{p_i}$ is in pixel coordinates; $\mathrm{P_i}$ is in world coordinates.

Applying equation (16) to n points, we get:

$$\begin{cases} -u_1\left(m_3 P_1\right) + m_1 P_1 = 0 \\ -v_1\left(m_3 P_1\right) + m_2 P_1 = 0 \\ \vdots \\ -u_n\left(m_3 P_n\right) + m_1 P_n = 0 \\ -v_n\left(m_3 P_n\right) + m_2 P_n = 0 \end{cases} \tag{17}$$

After Direct Linear Transformation (DLT) [5], equation (17) becomes:

$$Pm = 0 \tag{18}$$

$$P = \begin{bmatrix} P_1^T & 0^T & -u_1 P_1^T \\ 0^T & P_1^T & -v_1 P_1^T \\ & \vdots & \\ P_n^T & 0^T & -u_n P_n^T \\ 0^T & P_n^T & -u_n P_n^T \end{bmatrix}_{2n \times 12} \tag{19}$$

$$m = \begin{bmatrix} m_1^T \\ m_2^T \\ m_3^T \end{bmatrix}_{12\times 1} \tag{20}$$

Singular-value decomposition (SVD) of P gives the solution to the homogenous linear equation (18):

$$P \overset{SVD}{\rightarrow} U_{2n\times 12} D_{12\times 12} V_{12\times 12}^T \tag{21}$$

According to [3], the last column of V gives m. Repackage m and the result is denoted as:

$$\frac{M}{\rho} = \begin{bmatrix} a_1^T & b_1 \\ a_2^T & b_2 \\ a_3^T & b_3 \end{bmatrix}_{3\times 4} = K\begin{bmatrix} R & T \end{bmatrix} \tag{22}$$

Here ρ is a scalar. Based on equation (6), the intrinsic parameters are given by:

$$\begin{cases} \rho = \dfrac{\pm 1}{|a_3|} \\ u_0 = \rho^2 (a_1 \cdot a_3) \\ v_0 = \rho^2 (a_2 \cdot a_3) \\ \cos\theta = \dfrac{(a_1 \times a_3)\cdot(a_2 \times a_3)}{|a_1 \times a_3| \cdot |a_2 \times a_3|} \\ \alpha_u = \rho^2 |a_1 \times a_3| \sin\theta \\ \alpha_v = \rho^2 |a_2 \times a_3| \sin\theta \end{cases} \tag{23}$$

The extrinsic parameters are

$$\begin{cases} r_1 = \dfrac{(a_2 \times a_3)}{|a_2 \times a_3|} \\ r_2 = r_3 \times r_1 \\ r_3 = \dfrac{\pm a_3}{|a_3|} \\ T = \rho K^{-1} b \end{cases} \tag{24}$$

4.2. Camera Calibration Based on Nonlinear Model

The linear model does not take radial distortion into consideration, which is caused by imperfect lenses. The coordinates in the distorted image are displaced away or towards the image center. To model radial behavior[6]:

$$\begin{bmatrix} 1/\lambda & 0 & 0 \\ 0 & 1/\lambda & 0 \\ 0 & 0 & 1 \end{bmatrix} MP_i \to \begin{bmatrix} u_i \\ v_i \end{bmatrix} = p_i \tag{25}$$

$$d^2 = au^2 + bv^2 + cuv \tag{26}$$

$$\lambda = 1 \pm \sum_{p=1}^{3} K_p d^{2p} \tag{27}$$

Redefine Q as:

$$Q = \begin{bmatrix} q_1 \\ q_2 \\ q_3 \end{bmatrix} = \begin{bmatrix} 1/\lambda & 0 & 0 \\ 0 & 1/\lambda & 0 \\ 0 & 0 & 1 \end{bmatrix} M \tag{28}$$

Then equation (16) becomes

$$p_i = \begin{bmatrix} u_i \\ v_i \end{bmatrix} = \begin{bmatrix} \frac{q_1 P_i}{q_3 P_i} \\ \frac{q_2 P_i}{q_3 P_i} \end{bmatrix} = \frac{1}{\lambda} \begin{bmatrix} \frac{m_1 P_i}{m_3 P_i} \\ \frac{m_2 P_i}{m_3 P_i} \end{bmatrix} \tag{29}$$

Which is a nonlinear equation.

There are two methods to solve these nonlinear equations.

Method 1:

First, do not consider camera lens distortion which means setting λ to 1, and the initial estimation of the camera internal and external parameters are calculated by SVD with n physical points, then the nonlinear optimization algorithm is used to further fit the least square solution.

Method 2:

Method 1 treats all the parameters of the nonlinear model as parameter variables that need to be optimized, and the operation cost is expensive. In the method 2, the solution is simplified according to the characteristics of the radial distortion of the lens, and the operation efficiency is higher.

For models considering only radial distortion, the slope of a certain pixel on the image is constant regardless of the presence of lens distortion. So equation (29) can be written as:

$$\frac{u_i}{v_i} = \frac{\dfrac{m_1 P_i}{m_3 P_i}}{\dfrac{m_2 P_i}{m_3 P_i}} = \frac{m_1 P_i}{m_2 P_i} \tag{30}$$

Take n points into equation (30):

$$\begin{cases} v_1 \left(m_1 P_1 \right) - u_1 \left(m_2 P_1 \right) = 0 \\ v_2 \left(m_1 P_2 \right) - u_2 \left(m_2 P_2 \right) = 0 \\ \vdots \\ v_n \left(m_1 P_n \right) - u_n \left(m_2 P_n \right) = 0 \end{cases} \tag{31}$$

Since λ is removed, the above equation (31) are homogeneous linear, so we use singular value decomposition (SVD) to obtain the values of m_1 and m_2. After solving m_1 and m_2, the original nonlinear equations (29) are simplified to nonlinear equations with m_3 and λ as parameter variables. Finally, the nonlinear optimization algorithm is used to find the least square solution. Compared with method 1, fewer variables are needed to be fitted and the operation efficiency is higher.

4.3. Stereo Calibration

Stereo calibration is similar to single camera calibration and contains additional steps to get the relative rotation and translation between the two cameras and other useful information. After

single camera calibrations, we have the two cameras' extrinsic parameters, $R_1, R_2, T_1,$ and T_2. Then the relative rotation and translation matrices are shown as follows [3]:

$$\begin{cases} R = R_1 R_2^{-1} \\ T = T_1 - R_1 R_2^{-1} T_2 \end{cases} \tag{32}$$

4.4. Stereo Rectification

Rectification is based on the epipolar constraint [7], it makes it easier to find correspondence points between image pairs and to perform depth calculation. The traditional rectification method needs to do the image planes transformation so that the corresponding planes are coinciding [8]. There exist many variants of this traditional approach (e.g. [9-11]). This approach fails when the epipoles are located in the images since this would have to results in infinitely large images. [12] proposed a simple method to avoid this problem and guarantees minimal image size and works for all possible configuration.

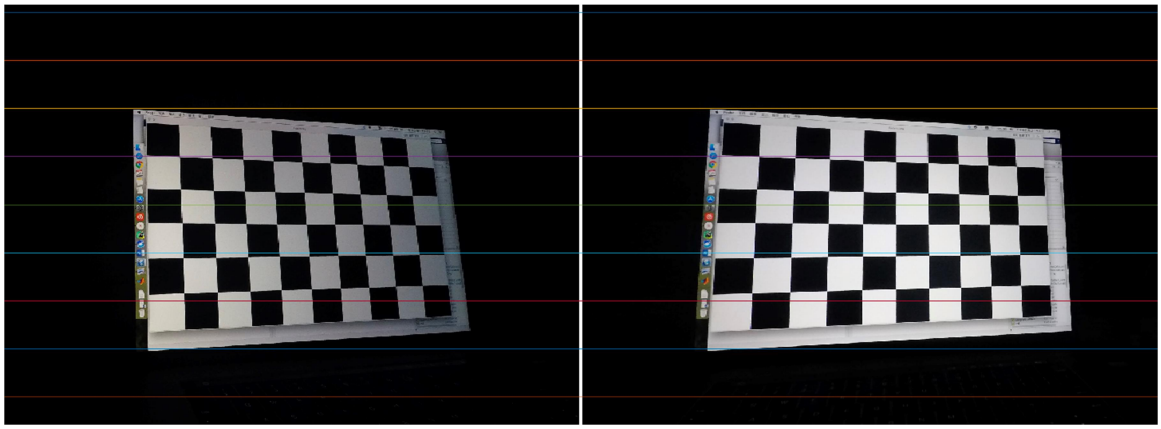

Figure 3. Image pair after stereo rectification

Figure 3 shows that correspondence points are horizontally aligned. Based on the measurement equations, we can easily calculate the depth and obtain additional 3D information about the scene.

4.5. Depth and Dimension Calculation

After camera calibration, image undistortion and rectification, the final step of this experiment is the calculation of the object's height, based on the modified measurement equations (9) and (10).

In this experiment, the stereo camera system is set with four different baselines, from 10cm to 40cm. The measured distance range is from 0.6m to 40m. The object to measure is a box with a chessboard on it. For distances from 0.6m to 9.6m, the step length is about 0.6m and the correspondence points were the chessboard's corner. For distance over 9.6m, the step length is about 6m and the correspondence points are picked from the edge of the object in the image.

CHAPTER 5

RESULTS AND ANALYSIS

5.1. Results

Camera calibration gives the intrinsic parameters of two cameras as shown in Table 1.

Table 1. Intrinsic parameters

Parameters	Left camera	Right camera
Radial distortion	[-0.2570, 0.0828]	[-0.2650, 0.0940]
Focal length in pixel	[1763.5, 1747.1]	[1758.9, 1743.7]
Principal point	[1471.2, 1116.2]	[1495.7, 1129.6]

Table 1 shows that the first component of the radial distortion is negative, this confirms that the cameras are set in the wide model, where images have barrel distortion.

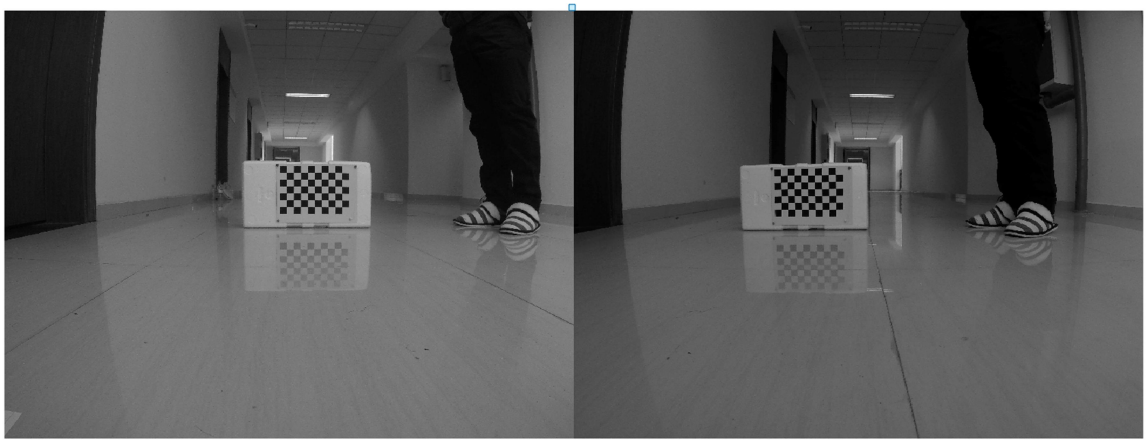

Figure 4. Samples of captured stereo images

Figure 4 shows that there exists serious barrel distortion, especially for the vertical lines which are more curved. After rectifying and removing distortion in the stereo images, the new intrinsic and extrinsic parameters are shown in Table 2.

Table 2. Intrinsic and extrinsic parameters, b=9.98cm

Parameters	Left camera	Right camera
Radial distortion	[6.2809e-05, -7.5997e-05]	[4.6459e-04, -8.9143e-04]
Focal length in pixel	[1765.1, 1765.0]	[1764.9, 1764.8]
Principal point	[1717.4, 1216.0]	[1717.7, 1216.0]
Translation of right camera	[-99.7644, -0.0013, -0.0323]	

After performing undistortion and rectification, the radial distortion parameters are reaching zero. Equations (9) and (10) are used to calculate the object's length in the vertical direction. Comparison with the actual values gives the error-distance curve shown in figure 5.

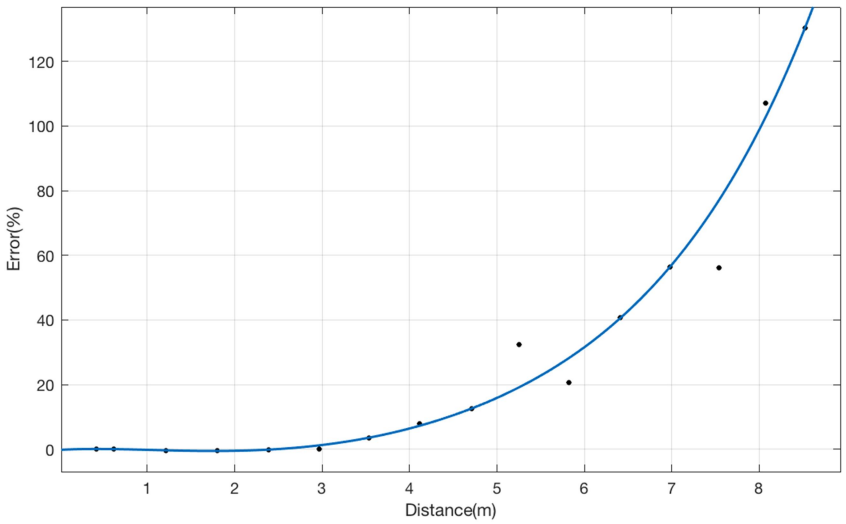

Figure 5. Error vs distance, b=9.98cm

By doing the same with other baselines, the following fitting curves are obtained:

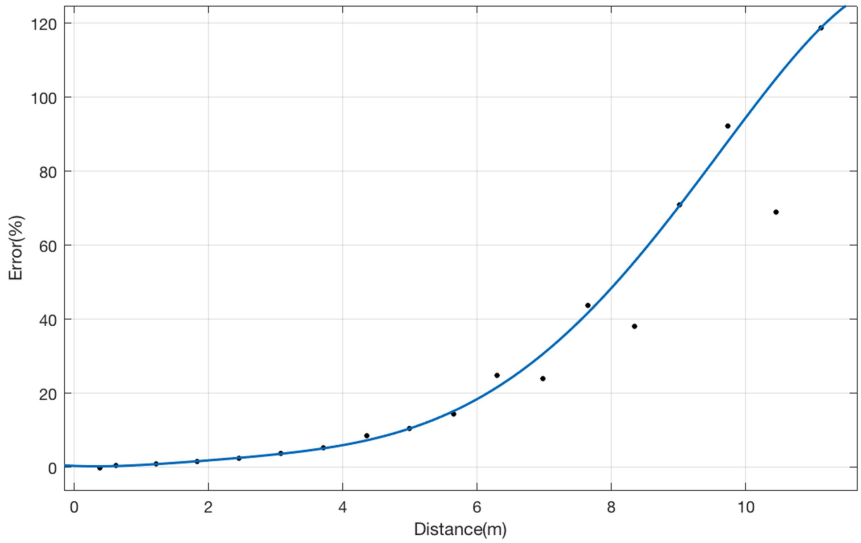

Figure 6. Error vs distance, b=19.81cm

In figure 6, the data points' x-axis step length is about 0.6m. In figure 7 and figure 8, the step length in the x-axis direction before 10m is 0.6m and becomes 3m or 6m after 10m.

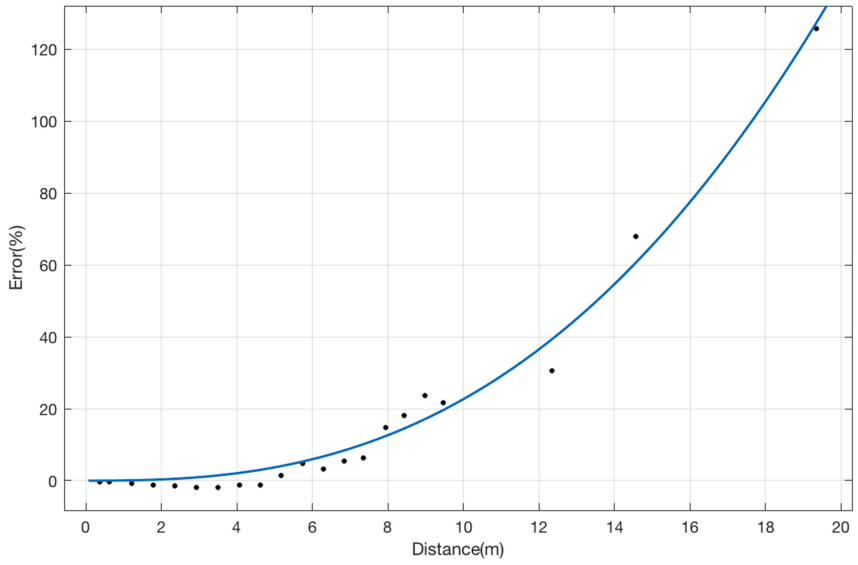

Figure 7. Error vs distance, b=29.92cm

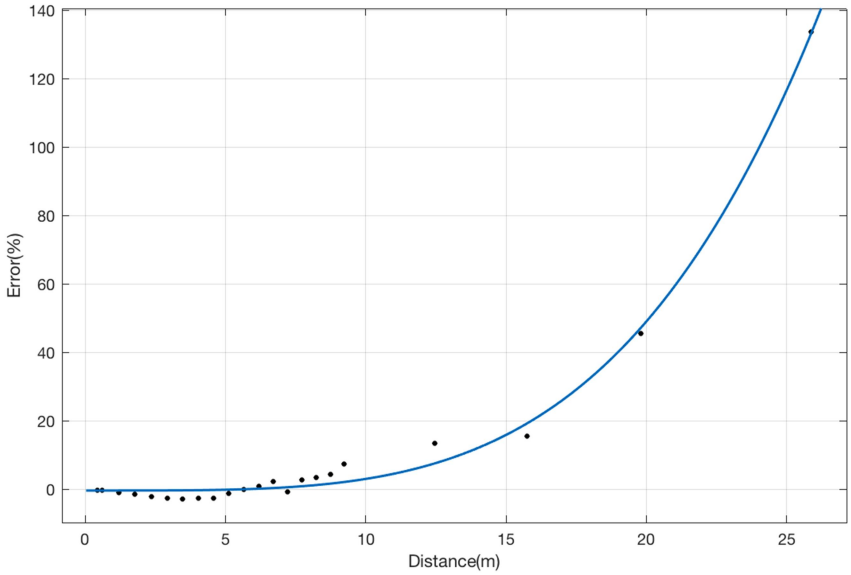

Figure 8. Error vs distance, b=39.84cm

5.2. Analysis

Figures 5-8 show that accuracy decreases with longer distance. In other words, the error in the height goes up in power of distance. This relationship converges with the equations mentioned in chapter 3. Meanwhile, with longer baseline, better accuracy is achieved at the same distance.

The accuracy obtained in this experiment is still not good enough. The best way to improve the accuracy is using a long focal length camera and doing sub-pixel points matching.

CHAPTER 6

CONCLUSION AND FUTURE WORK

In this project, the baseline's effect of stereo vision systems is studied using error analysis. The error increases in power of the distance and is inversely proportional to the baseline. To confirm this relationship, a measurement experiment is conducted. The methodology of this experiment is explained in detail. Some parts of the experiment, such as camera calibration and rectification can be applied to other applications.

Future work is includes investigating the image correspondence problem in stereo vision. The aim is to find one specific point's correspondence at sub-pixel level so that the calculations can be more accurate.

REFERENCES

[1] De la Escalera, A., J.M. Armingol, and M. Mata, *Traffic sign recognition and analysis for intelligent vehicles.* Image and vision computing, 2003. **21**(3): p. 247-258.

[2] Luhmann, T., et al., *Close range photogrammetry*. 2007: Wiley.

[3] Hartley, R. and A. Zisserman, *Multiple view geometry in computer vision*. 2nd ed. 2003, Cambridge, UK ; New York: Cambridge University Press. xvi, 655 p.

[4] Rumelhart, D.E., G.E. Hinton, and R.J. Williams, *Learning internal representations by error propagation*. 1985, California Univ San Diego La Jolla Inst for Cognitive Science.

[5] Dainis, A. and M. Juberts. *Accurate remote measurement of robot trajectory motion*. in *Robotics and Automation. Proceedings. 1985 IEEE International Conference on*. 1985. IEEE.

[6] Zhang, Z., *A flexible new technique for camera calibration.* IEEE Transactions on pattern analysis and machine intelligence, 2000. **22**(11): p. 1330-1334.

[7] Fusiello, A., E. Trucco, and A. Verri, *A compact algorithm for rectification of stereo pairs.* Machine Vision and Applications, 2000. **12**(1): p. 16-22.

[8] Ayache, N. and C. Hansen. *Rectification of images for binocular and trinocular stereovision*. in *Pattern Recognition, 1988., 9th International Conference on*. 1988. IEEE.

[9] Faugeras, O., *Three-dimensional computer vision: a geometric viewpoint*. 1993: MIT press.

[10] Papadimitriou, D.V. and T.J. Dennis, *Epipolar line estimation and rectification for stereo image pairs.* IEEE transactions on image processing, 1996. **5**(4): p. 672-676.

[11] Loop, C. and Z. Zhang. *Computing rectifying homographies for stereo vision*. in *Computer Vision and Pattern Recognition, 1999. IEEE Computer Society Conference on.* 1999. IEEE.

[12] Pollefeys, M., R. Koch, and L. Van Gool. *A simple and efficient rectification method for general motion*. in *Computer Vision, 1999. The Proceedings of the Seventh IEEE International Conference on*. 1999. IEEE.